

Fundamental reflectivity and electronic structure of NiBr₂ and NiCl₂ insulators

I. Pollini

*Dipartimento di Fisica, Università di Milano, Gruppo Nazionale di Struttura della Materia
del Consiglio Nazionale delle Ricerche, Italy
and Laboratoire d'Utilisation du Rayonnement Electromagnétique,
Université de Paris-Sud, Orsay, France*

J. Thomas, G. Jezequel, and J. C. Lemonnier

*Laboratoire de Spectroscopie, Université de Rennes, Rennes, France
and Laboratoire d'Utilisation du Rayonnement Electromagnétique,
Université de Paris-Sud, Orsay, France*

R. Mamy

*Laboratoire de Physique des Solides, Université P. Sabatier, Toulouse, France
and Laboratoire d'Utilisation du Rayonnement Electromagnétique,
Université de Paris-Sud, Orsay, France*

(Received 25 May 1982)

The fundamental reflectivity of NiBr₂ and NiCl₂ has been measured over the energy range 2–11 eV from 300 to 30 K with the use of synchrotron radiation. The imaginary part of the dielectric constant ϵ_2 has been determined at 30 K by means of the Kramers-Kronig technique. The structure in the complex optical spectra of nickel halides is interpreted in terms of charge-transfer transitions, orbital promotions, excitons, and direct allowed interband transitions at the symmetry points Γ , Z , and F , and along symmetry lines Λ , B , and Γ - L of the Brillouin zone. The energy gap is assigned to $\Gamma_3^- \rightarrow \Gamma_1^+$ transitions at the zone center, both in NiBr₂ (7.90 eV) and NiCl₂ (8.70 eV). Finally, the interpretation of the satellite exciton at 6.5 eV in NiBr₂ (30 K) is discussed.

I. INTRODUCTION

Transition-metal halides (TMH) are of fundamental interest in solid-state physics because they belong to the restricted group of materials for which one-electron band theory is inadequate to explain the electronic properties.¹ The presence of unfilled localized $3d$ shells has a significant influence on their optical properties, whose understanding is of considerable interest in order to determine their electronic structure. Previous studies made on the oxides^{2,3} and halides⁴⁻⁷ of iron-group transition metals have shown that these compounds have complex optical spectra, whose interpretation has been first attempted by means of an intermediate picture involving a mixture of one-electron bands and localized states, as the one proposed by Adler and Feinleib⁸ to order the states of NiO. More recently, self-consistent band structures for the nickel halides⁹ and Co, Fe, and Mn chlorides¹⁰ have been calculated by the intersecting-spheres model. This model should provide fairly accurate results for the valence band and low-lying conduction levels and allow at least a

qualitative interpretation of the optical and x-ray spectra of TMH.^{11,12} In fact, it was found that even in the exemplary case of MgCl₂ (Ref. 9) the calculated forbidden gap, which is unambiguously identified, is rather underestimated by about 2–3.2 eV, according to the approximation used for the exchange potential. The gap identification is still more complicated in the case of NiX₂ ($X = \text{Cl, Br}$) and the other halides considered by us,¹³ because of the simultaneous presence of the empty s and d states of the metal ion. It was the consciousness of these difficulties, together with the knowledge of the oxide tradition, which gave us the confidence to reconsider the reflectivity of NiX₂ in the fundamental absorption region, in order to sort peaks due to excitons and those due to Van Hove singularities in the interband density of states. In this work we describe the fundamental reflectivity of NiBr₂ and NiCl₂ in the energy range 2–11 eV down to 30 K, obtained with the use of synchrotron radiation at the Laboratoire d'Utilisation du Rayonnement Electromagnétique (LURE) (University of South Paris). This is part of a more complete study of the funda-

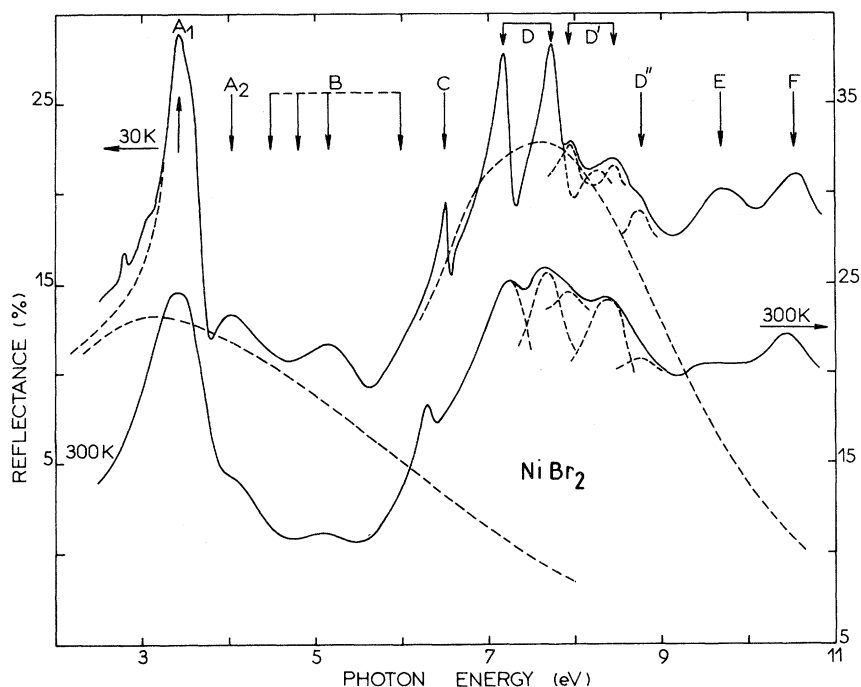


FIG. 1. Reflectance spectra of NiBr_2 crystals at 300 and 30 K. The major structures discussed are designated by capital letters *A* through *F*. The nonresonant background level is indicated by the dashed line in the region of peaks *C* and *D* in the spectrum at 30 K.

mental optical properties of TMH between 2 and 31 eV which will be reported shortly.¹³ Of the three halides studied, NiX_2 revealed reflectance data richer in structure than either CoX_2 or FeX_2 . For this reason, and since an understanding of NiX_2 may provide a basis for interpreting the spectra of the other compounds, we will treat their spectra separately. In Secs. II and III we present the techniques employed in order to measure near-normal incidence reflectance data of single-crystal specimens and examine the experimental results. In Sec. IV we propose an interpretation of the sharp structures observed in terms of charge transfer and orbital promotion transitions by means of a mixed-band localized-state model and of the interband transition with the aid of the one-electron-band scheme of NiCl_2 .¹⁰ Finally Sec. V contains the conclusions along with some considerations on the forthcoming work.

II. EXPERIMENTAL PROCEDURE

Synchrotron radiation from the 0.54-GeV storage ring anneau de collision d'Orsay (ACO) at the LURE was used as a light source. The monochromator delivers a continuous spectrum, very stable, between 2 and 31 eV, with a resolution of about 8 Å and a flux of 10^9 photons/Å sec at 5 eV. Filters of LiF and MgF_2 were used in the appropriate regions

in order to eliminate the higher orders. The detection was made by means of a 6256S EMI photomultiplier provided with a salicylate phosphor. The advance of the monochromator (4-Å step), as well as the signal recording, was controlled by system based on a 4051 Tektronix computer. In practice, the incident radiation intensity and the reflected light are registered and compared by the calculator, which gives the reflectivity at the incidence angle ($\leq 20^\circ$) directly. Single crystals of NiCl_2 and NiBr_2 were obtained from the vapor phase by the dynamical transport method. Because they are hygroscopic, sample preparation has been made in an atmosphere of dry nitrogen with the aid of a glovebox directly attached to the reflectometer. Ionic pumps and some flashes of titanium on cold traps provided an ultimate pressure of the order of 10^{-10} -mm Hg in the cryostat. A thermoregulated helium-flow cryostat was employed for measurements at different temperatures down to 30 K. The temperature was permanently monitored by means of a platinum resistance thermometer.

III. RESULTS

Figures 1 and 2 show detailed reflectance spectra of NiBr_2 and NiCl_2 measured at 300 and 30 K. These spectra are very similar in many aspects: There are main groups of peaks, which are located

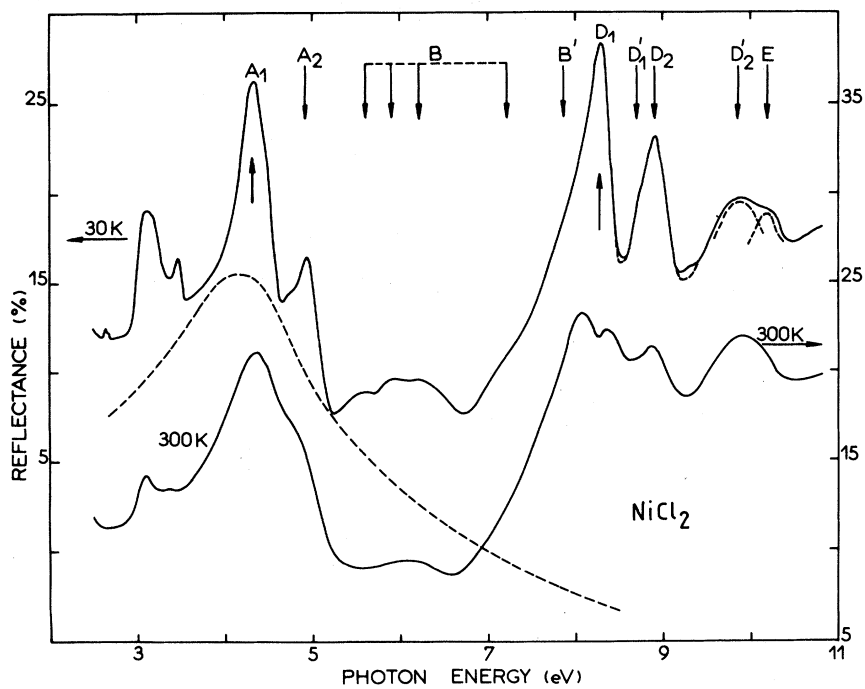


FIG. 2. Reflectance spectra of NiCl_2 crystals at 300 and 30 K. The major structures discussed are designated by capital letters *A* through *E*.

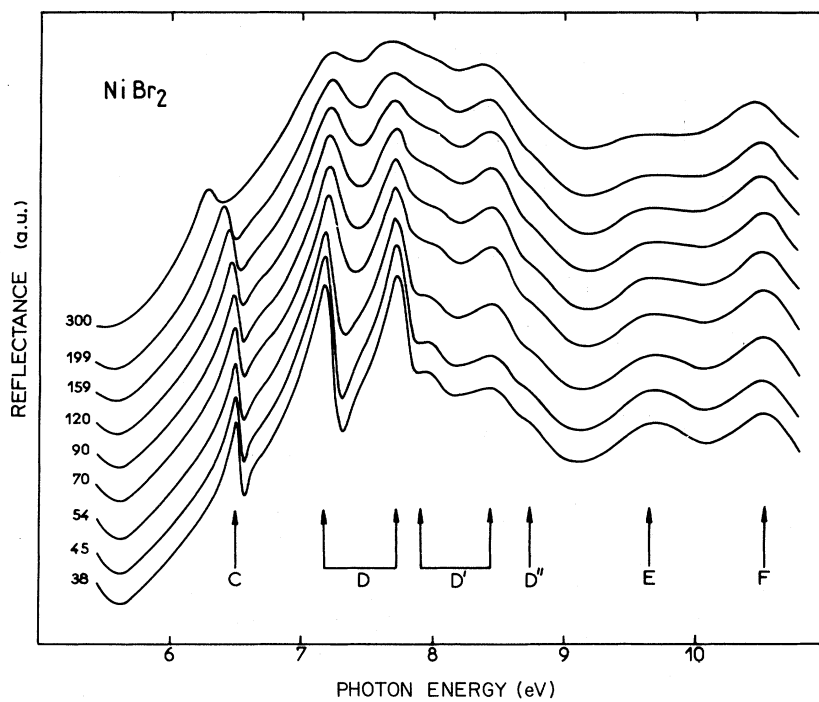


FIG. 3. Reflectance spectra of NiBr_2 taken at fixed temperatures between 300 and 30 K.

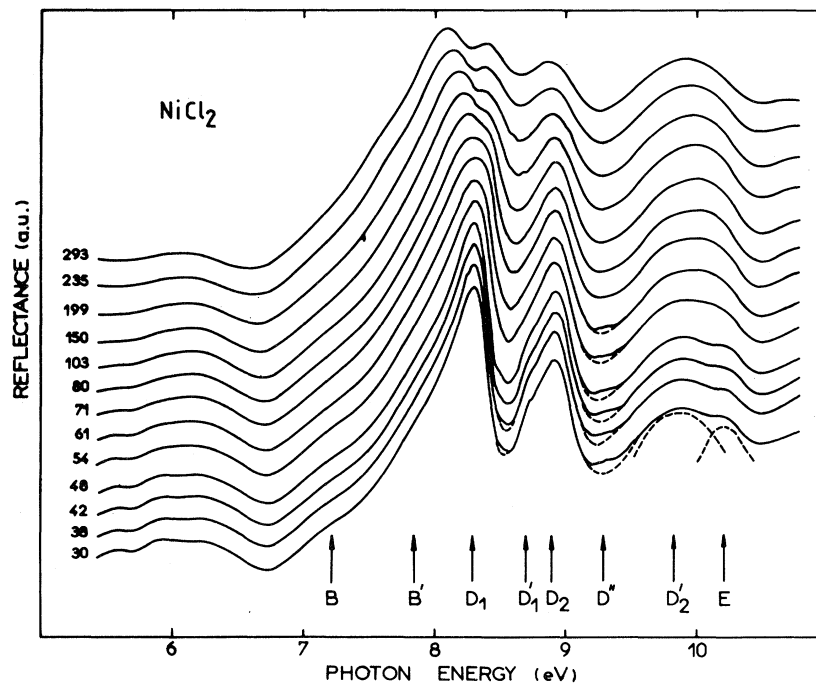


FIG. 4. Reflectance spectra of NiCl_2 taken at fixed temperatures between 293 and 30 K.

in the low-energy region (A_1 and A_2) and in the high-energy region (C, D, D', D'', E, F) separated by a weak and broad band (B), which shows a weak structure at low temperature. The sharp peak C located at 6.50 eV in NiBr_2 (30 K) and the preceding weak hump around 5.94 (see Fig. 1) are observed for the first time in NiCl_2 (30 K) like faint, but genuine, oscillations superimposed on the edge of the peak D_1 around 7.15 (B) and 7.81 eV (B') (see Fig. 2). The peak C in NiBr_2 and the peaks D in both crystals (the common letter D does not necessarily mean that both peaks have the same origin) sharpen and shift in general, but not always, to higher energies on lowering the temperature. Moreover, they present in the spectra at 30 K the characteristic asymmetry and antiresonance typical of excitonic transitions: i.e., the peaks at 6.50, 7.15, and 7.60 eV in NiBr_2 and 8.28 and 8.92 eV in NiCl_2 are followed by antiresonance dips around 6.55 and 7.30 eV in NiBr_2 and 8.50 and 9.25 eV in NiCl_2 which go below the average level of the band continuum. Further, we observe, always in the region of peaks D , structures D' which can be easily followed in the spectra taken at different temperatures (see Figs. 3 and 4) and show up around 7.90 and 8.44 (D') and 8.74 (D'') eV in NiBr_2 and 8.70 (D'_1) and 9.26 (D'') eV in NiCl_2 . The peaks denoted by letters E and F do not show such a rapid sharpening as the temperature is decreased. It is in general found that peaks

in the bromides (and NiBr_2) are slightly narrower than in chlorides (and NiCl_2).¹³ This fact can be understood if one considers that in the NiX_2 crystal structure¹⁴ (CdCl_2 -type structure; point group D_{3d}) the halogen atoms are arranged on almost regular octahedra surrounding the Ni atom, but the "cage" in which Ni^{2+} is contained is larger when the ligands are bromine ions. This results on the average in a weaker electron-phonon interaction, which means narrower bands. The Kramers-Kronig relations are applied to the spectra observed as far as 31 eV to obtain the dielectric constants which describe the optical properties. The values of the imaginary parts ϵ_2 are reported in Figs. 5 and 6, together with the proposed assignments to transitions involving d states (see Fig. 7) and valence-conduction bands (see Fig. 8).

IV. DISCUSSION

We present first the main excitation mechanisms based on a mixed localized-band model, as the one first used by Adler and Feinleib,⁸ together with a discussion of the role of excitons in these ionic crystals. Then we will attempt to interpret the high-energy optical absorption in terms of the available electronic band structure.^{9,10} In Fig. 7 the electronic states of NiBr_2 are summarized schematically. The valence band of NiBr_2 (or else of NiCl_2 in the corresponding scheme, which is not shown) has been

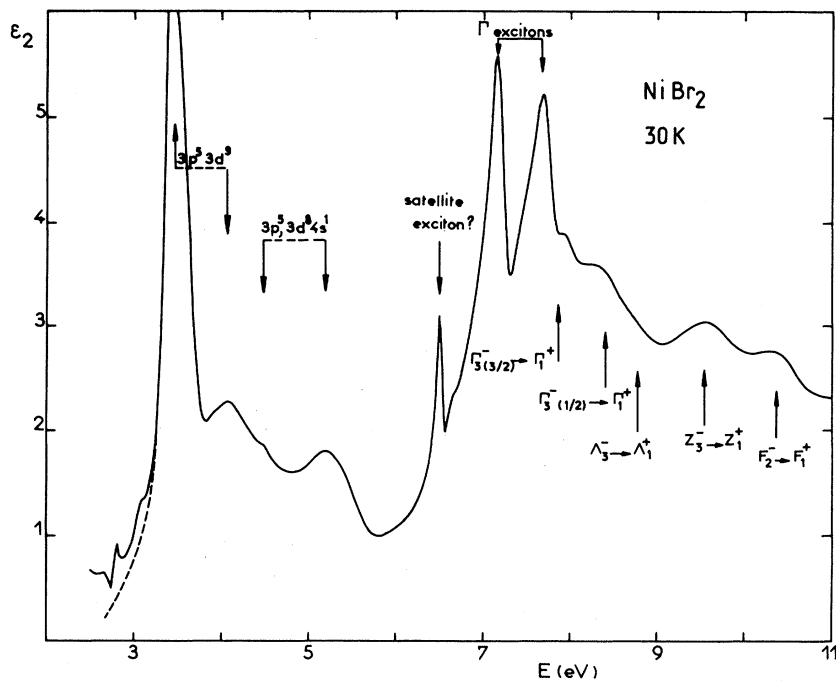


FIG. 5. Imaginary part of the dielectric constant of NiBr_2 together with the proposed assignments, according to the localized model introduced in the text and the band structure, as inferred from experiment by analogy with Fig. 6.

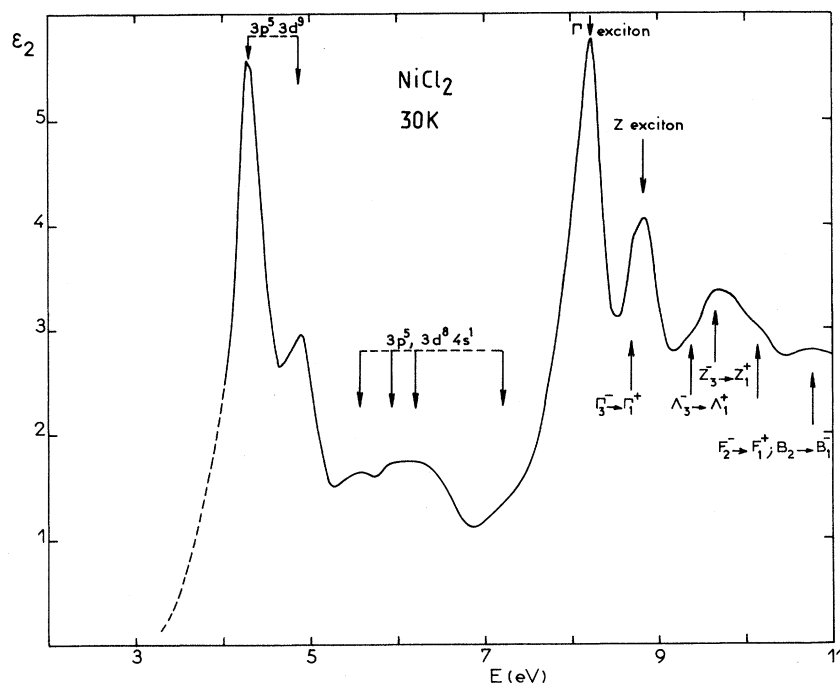


FIG. 6. Imaginary part of the dielectric constant of NiCl_2 together with the proposed assignments, according to the localized model introduced in the text and the band structure of Ref. 10.

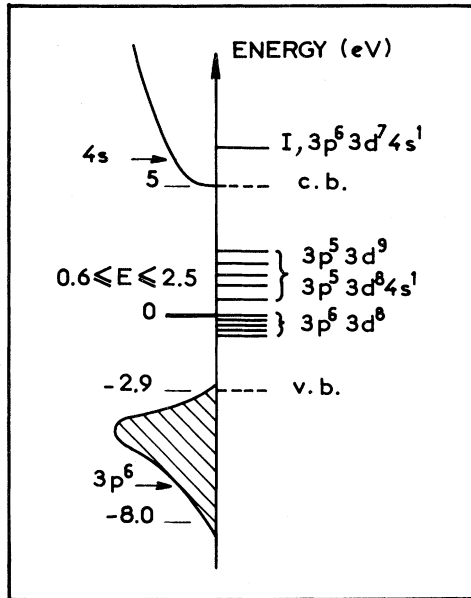


FIG. 7. Electronic states of NiBr₂ as deduced from optical and photoemission spectra. One-electron bands are shown to the left of the vertical line, and localized states to the right. The states which are filled at $T=0$ are shaded. On the right edge are shown the excited states which can be reached by dipole transitions from either the valence band (charge transfer) or the ground state 3F (orbital promotion) of Ni²⁺ ion.

drawn by considering the x-ray photoemission spectra of Ref. 12. X-ray data reported by various authors^{11,12} indicate that the Br 4*p* and Cl 2*p* states lie below the Ni 3*d* states and also that the *p* band is approximately 5 eV wide, while the 3*d* states are less than 1 eV in width. This means that in the forbidden gap between the filled *p*-type (halogen) valence band and the *s*-type (metal) conduction band, there is a set of localized, partially filled 3*d* states, among which localized *d*-excitons (crystal-field transitions) occur. The following types of transitions are further expected: (i) An electron can be excited from a localized 3*d* state into the 4*s* band (orbital promotion transition). For example, in NiO (Ref. 15) the structure observed in reflectance and electroreflectance^{16,17} around 4 eV was assigned to this type of transition. This is possible in a crystal, considering the mixing of the orbitals of the metal ion with those of the halogen, which can be appreciable, as well as the hybridization of orbitals within the nickel ions. For the same reasons the sharp structure C in NiBr₂ could also be assigned to the transition $3d^8 \rightarrow 3d^7 4s^1$ between *d* levels and the level I of Fig. 7. (ii) An electron can be excited from the *p* band into a localized 3*d* state. (iii) An electron can be raised from a 3*d* state of one Ni²⁺ ion into a 3*d*

state of another Ni²⁺ ion, creating a (Ni⁺, Ni³⁺) pair. For NiO,¹⁵ these transitions occur in the energy range 6–8.5 eV, overlapping the conduction band. In NiBr₂ these transitions are probably in competition with the much stronger *p*→*s* transitions and may be buried under the large absorption structure which extends between 6 and 10 eV. (iv) One-electron transitions can occur between *p* and 4*s* bands: These transitions give the value of the forbidden gap. All the transitions presented above should give rise in a crystal to pronounced optical structure.^{2,18} A discussion of our optical spectra in

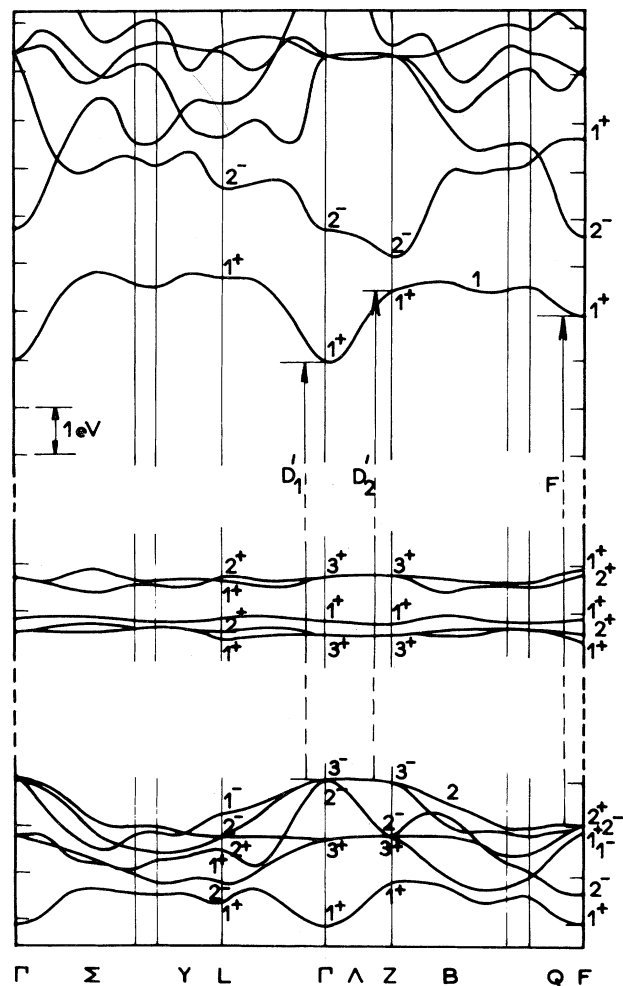


FIG. 8. Energy bands of NiCl₂ according to Antoci and Mihich (Ref. 10) when the Slater approximation for the exchange potential was used. It should be noted that the forbidden gap has been purposely increased in order to agree with the experimental values for interband transitions considered at the zone center and the main symmetry points.

terms of these transitions will be proposed below. The peaks *A* have been formerly interpreted as arising from charge-transfer transitions ($p \rightarrow d$ type) by various authors^{5,6} and more recently by Simonetti and McClure.¹⁹ In Ref. 6 definite reasons were given for the assignments of the low-energy allowed transitions (peaks *A* and *B*) to charge-transfer transitions in NiX_2 instead of orbital promotion ($d \rightarrow s$ type) transitions as in NiO, although we must consider they are likely to overlap considerably in this energy range. Besides, other authors^{5,19} emphasize that charge-transfer transitions are only possible to e_g orbitals: This would cause some difficulty for the assignments of the broad structure B (which the present reflectance data and thermorefectance measurements⁶ reveal to be structured at low temperature), which is not even interpreted by Sakisaka *et al.*⁵ In fact we must consider that both $p^5 3d^9$ and $p^5 3d^8 4s$ are possible, nearly degenerate, final configurations. This would still permit the interpretation of peaks *B* to charge-transfer transitions of the kind $p^6, 3d^8 \rightarrow p^5, 3d^8 4s$,¹ in conformity with the assignment given for NiO (Ref. 20) (see Fig. 7). Now we discuss the excitonic region of the spectra, where the sharp peaks *C* and *D* appear. The peak *C* in NiBr_2 was not assigned by Sakisaka *et al.*⁵ and was then generally referred to as an exciton (like peaks *D*) on the basis of the behavior with temperature in reflectance and thermorefectance measurements.⁶ It is our wish to try more specific attributions of these excitonic peaks, after a few preliminary comments. If it is true that charge-transfer transitions tend to exhaust around the minima observed between 5.5 and 6.5 eV in NiX_2 (see Figs. 1 and 2), this means that new kinds of transitions (partially overlapping with the foregoing $p \rightarrow d$ transitions) can start in this energy region, beginning to build the strong structured band extending from 5.5 to 9 eV. It is reasonable to assign most of this part of the spectrum to the $p \rightarrow s$ interband transitions, although other types of transitions may participate to the ultraviolet absorption. In spite of widespread agreement^{5,6,10} about the nature of these transitions, the identification of the forbidden gap has not yet been given (also for lack of convincing measurements), though Antoci and Mihich suggested¹⁰ for transition-metal (TM) chlorides a values around 8.5 eV. The likely appearance of excitons interspersed with interband effect in TMH can be mainly associated with their relatively small dielectric constant $\epsilon_{\text{eff}} = 3-4$ (Ref. 13) and relatively large lattice distances. Therefore, the Coulomb interaction is still very effective and should have approximately a strength intermediate between alkali halides and silver halides.²¹ A convenient criterion for TMH ionicity can be the ion net charge values, which range from 0.90 to 0.70

from MnX_2 to NiX_2 ,²² and must be compared to the values around 0.90–0.98 for alkali halides.²³ These figures inform us of the scale of ionicity of the TMH and about the relative weight of excitonic-interband effects. Thus we look for exciton resonances well separated from the parent interband edges and expect also NiX_2 exciton resonances to be degenerate with the continuum of states as occurs in alkali iodides²⁴ and silver halides.²⁵ In conclusion, we think that d -electron states in the forbidden gap introduce new kinds of transitions (unusual for alkali halides) but do not affect substantially the interband energy distance. In fact, the only relevant effect of the presence of d levels on the overall band structure seems to be a downward shift of high conduction bands ($\Gamma_3^+, Z_3^+, L_2^+, F_2^+$) and an upward shift of F_1^+ valence levels¹⁰ (see also Fig. 8).

Coming back to the peaks *D* in NiBr_2 (Fig. 1), we observe that they sharpen more rapidly than the nearby structures *E* and *F* as the temperature is lowered and are very similar to the parabolic excitons in KBr and NaBr,²⁴ associated with the lowest spin-orbit split M_0 -type edge at the point Γ of the Brillouin zone. The presence of the characteristic asymmetry and antiresonance of the excitonic peak and the splitting of 0.55 eV give a way of identifying the forbidden gap, which in NiBr_2 is at 7.9 ± 0.05 eV (first component of peaks *D'*) and is associated with the direct transition $\Gamma_3^- \rightarrow \Gamma_1^+$. A similar situation is depicted in Fig. 2, where two strong excitonic peaks D_1 and D_2 are followed by two structures D'_1 and D'_2 at 8.70 ± 0.05 and 9.82 ± 0.05 eV, which can be associated with the parent interband transitions $\Gamma_3^- \rightarrow \Gamma_1^+$ and $Z_3^- \rightarrow Z_1^+$. In this case no spin-orbit splitting is observed (≤ 0.1 eV).

As we can see, the excitonic region of the nickel halides is very similar to that of the isotropic alkali halides (rocksalt and cubic structures) even though it might be reasonable that in our layered structures the exciton could be more localized to individual layers and present bidimensional effects. Thus it may be in order to consider briefly the optical spectra in the anisotropic insulator CdI_2 (same crystal structure as TM bromides) in order to look for empirical clues for bidimensional effects, which could also affect the optical spectra of nickel halides. We see that the absorption²⁶ and reflectivity²⁷ spectra of CdI_2 show evidence of strong interband scattering and a most remarkable structure around 6 eV, with peaks X_3 and X_4 (see Ref. 26), which, even at 300 K, are well separated by a sharp symmetrical antiresonance of the form predicted by Fano's theory.²⁸ The present interpretation assigns the X_3 and X_4 excitons to the quasidegenerate transitions $np^6 \rightarrow np^5(n+1)s$, $np^5(n+1)p$ split by spin-orbit interaction. Because the exciton structure X_3 and X_4

has been observed both for $\vec{E} \perp \vec{C}$ and $\vec{E} \parallel \vec{C}$, it is concluded that the excitons in CdI_2 are not of bidimensional character.²⁹ While this example does not exclude entirely this possibility for our materials as well, nevertheless it gives us one more reason for comparing the TM halides to the alkali halide family.

The peak *C* in NiBr_2 is of difficult interpretation. We still observe the characteristic excitonic asymmetry and antiresonance dip into the $p \rightarrow d$ charge-transfer background, typical of the Γ^- excitons, but its intensity is lower than that of either Γ excitons or charge-transfer bands *A*, both of which involve p -type valence states. This would seem to indicate a different origin for the peak *C* and justify a different exciton-phonon coupling. Thus we may assign this sharp peak (half width ≈ 0.1 eV at 30 K) to an exciton associated with orbital promotion transitions to the partially hybridized *S* orbital²⁰ (level I of Fig. 7). One may wonder about the intensity gain of the atomically forbidden $d \rightarrow s$ transition when it occurs between Bloch levels. Of course the description of the excited electronic states of a crystal by band theory neglects the change in the Coulomb energy (Hartree-Fock approximation) introduced when an electron is transferred from the valence to the conduction band, but if the Coulomb terms are properly modified, the energy levels of the crystals are obtained. Thus we can expect some hybridization with odd-parity states also for the lowest conduction bands. Furthermore, a second explanation may be given for the oscillator strength of the $d \rightarrow s$ transition. Because the associated exciton (peak *C*) is degenerate with the background of the preceding *A* and *B* bands, its line shape gets the typical asymmetry caused by the interference between the exciton resonance and the scattering background^{28,30} and a large fraction of the oscillator strength of allowed charge-transfer transitions can be transferred to the exciton resonance.

However, the explanation offered for the peak *C* in NiBr_2 in the framework of the mixed model, while suggestive, does not explain why the excitation mechanism is not active in NiCl_2 . For this reason we prefer the alternative interpretation, which has also the advantage of being more in keeping with the experimental data. The bromine doublet *D* is known to derive from interband edges excitons $(\frac{3}{2}, \frac{1}{2})$ and $(\frac{1}{2}, \frac{1}{2})$, where the first members in the parentheses indicate the total angular momentum *j* of the hole and the second specifies *j* of the electron. Onodera and Toyozawa³¹ have shown that a triplet exciton state of total angular momentum $J=2$ can exist below the exciton state $\Gamma(\frac{3}{2}, \frac{1}{2})$, with $J=1$. While in chlorides the triplet-singlet state separation would be very small, in bromides this triplet exciton state

would be well separated from the lower energy Γ exciton so that it should be possible to observe it. In fact this satellite exciton was observed at low temperature in CoBr_2 and FeBr_2 as well.¹³ While we wish to discuss this point in more detail in a forthcoming paper, we want to make some more considerations now, in order to clarify the present suggestion. If this interpretation is correct, not only would the energy of the triplet state be lower than the singlet state, but also its width would be less, on account of the longer lifetime of the excited state. In fact, the transition to the singlet ground state would be forbidden by the spin-selection rule, which can be slightly relaxed if spin-orbit coupling is taken into account. Besides, while the direct process to triplet state $J=2$ is forbidden, the indirect transition assisted by phonons is possible.³¹ The mechanism for the intensity gain of the excitonic transition to the triplet state would still be in accord with Fano's theory.²⁸ This would further explain why this peak is difficult to observe in the case of alkali halides, where no strong background exists below the exciton doublet.

In the following we make a joint discussion of NiBr_2 and NiCl_2 by considering the band structure calculated by Antoci and Mihich by the intersecting-spheres model in the Slater approximation for the exchange potential.¹⁰ The positions of conduction and valence bands have been properly shifted to put the calculated gap in coincidence with the measured gap of nickel halides (Fig. 8). In order to compare the results obtained from the theory of direct transitions with the experimental results of NiX_2 over 7 eV, we present in Figs. 5 and 6 the dielectric function $\epsilon_2(E)$, whose structure is basically determined by the joint density of states. We also have indicated the lower-energy attributions based on the mixed-localized-state model introduced in Fig. 7. In NiBr_2 (Fig. 5) we see that the optical spectrum is interpreted by transitions from the highest valence band Γ, Z, F to the lowest conduction band. The shoulders and peaks in the density of states at critical points are clearly present in the experimental curves (see also Fig. 1). There are shoulders *D'* around 7.90 and 8.44 eV corresponding to the transitions $\Gamma_{3(3/2)}^-, \Gamma_{3(1/2)}^- \rightarrow \Gamma_1^+$, a weak structure *D''* assigned to the transitions $\Lambda_{\bar{3}}^- \rightarrow \Lambda_1^+$ along the symmetry line Λ and higher-energy peaks (*E, F*) attributed to $Z_{\bar{3}}^- \rightarrow Z_1^+$ and $F_{\bar{2}}^- \rightarrow F_1^+$. Further confirmation of our interpretation can be obtained by the observation of the spin-orbit splitting associated with the p -like valence-band states in the transitions at energies below the energy gap and ascribed to Γ excitons (peaks *D*). In NiCl_2 (Fig. 6) the strong peaks *D*₁ and *D*₂ of Fig. 2, broadened by spin-orbit interaction, have a halfwidth of about 0.5 eV in

analogy with alkali chlorides,²⁴ which have the same average width but show spin-orbit splitting of ~ 0.1 eV.

We assign these peaks to Γ and Z excitons associated with the interband edges $\Gamma_3^- - \Gamma_1^+$ and $Z_3^- - Z_1^+$ at 8.72 eV and around 9.73 eV, respectively. The high-energy tail of the peak E around 10.7 eV is ascribed to both critical point $F_2^- \rightarrow F_1^+$ transitions and $B_2 \rightarrow B_1$ transitions along the symmetry line B of the zone. We remark that only the valence and conduction bands near the energy gap are considered here, as they are the most reliable in interpreting most of the scattering structure. Note also that beyond the energy gap at 8.70 eV the lowest interband energy distance is found at the somewhat overestimated Z point at 10.20 eV. The shoulder around 9.30 eV can be then assigned to $\Lambda_3^- \rightarrow \Lambda_1^+$ transitions. If this assignment is correct we obtain the binding energies $B_\Gamma \simeq 0.50$ eV and $B_Z \simeq 0.89$ eV for Γ and Z excitons, which are not far from the binding energies of Γ and L excitons in alkali chlorides [e.g., for KCl, $B_\Gamma \simeq 0.8$ eV and $B_L \simeq 0.85$ eV (Ref. 32)].

As a concluding remark, we note that structures D_2' and D_2 are attributed, respectively, to a critical-point transition at Z and its associated exciton. Ac-

cording to the available band structures for NiCl_2 , it seems difficult to assign the D_2' structure to a critical-point transition of type M_0 for energy reasons (see Fig. 8). This would allow one to attribute the peak D_2 to a metastable (but not extra) exciton in analogy with alkali halides and solid rare gases. Yet in our crystal the interband critical point assigned to D_2' seems to be either an M_1 or M_2 , making the Z exciton a hyperbolic exciton in the sense of Philipps.³² According to his analysis these excitons have been identified in NaI, KCl, KBr, KI, RbCl, RbBr, and RbI.³³ However, the existence of hyperbolic excitons has caused some controversy among theorists.³⁴⁻³⁷ In particular, the NiCl_2 Z exciton does not appear to show the calculated saddle-point line shape,³⁷ although its line shape is similar to that of L excitons in most alkali halides.³³ While this problem is still rather unsettled, some experimental evidence seems to have been mounting in favor of saddle-point excitons, for example at the $\Lambda_3 \rightarrow \Lambda_1$ transitions of cubic semiconductors.³⁸ Finally, in order to summarize the main results, we report in Table I the experimental values of energy (eV) for the structures of $\epsilon_2(E)$ and R observed at 30 K. The relevant transitions considered in Figs. 7 and 8 are also indicated.

TABLE I. Energies of the peaks in the imaginary part of the dielectric constant ϵ_2 and reflectivity R observed at 30 K in layered NiBr_2 and NiCl_2 crystals (CdCl₂ type). Experimental energies are compared with the theoretical values (from Ref. 10), and symbols for the interband energy differences at or near symmetry points are also reported.

Labeling of the peaks	NiBr_2			NiCl_2			
	Expt. $R(30\text{ K})$	Expt. $\epsilon_2(30\text{ K})$	Theor.	Expt. $R(30\text{ K})$	Expt. $\epsilon_2(30\text{ K})$	Theor.	
A	A_1	3.42	3.46	$3p^6 \rightarrow 3p^5 3d^9$	4.31	4.28	$3p^6 \rightarrow 3p^5 3d^9$
	A_2	4.05	4.04		4.93	4.90	
B	B_1	4.48	4.54	$3p^6 \rightarrow 3p^5 3d^8 4s^1$	5.57	5.59	$3p^6 \rightarrow 3p^5 3d^8 4s^1$
	B_2	4.81			5.92	5.92	
	B_3	5.15	5.27		6.23	6.21	
	B_4	5.94			7.15	7.20	
B'				7.81			
C		6.50	6.56				
D	D	7.15	7.17	Γ excitons			
		7.70	7.72				
	D'	7.90	7.90	$\Gamma_3^-(\frac{3}{2}) - \Gamma_1^+$ gap			
		8.44	8.39	$\Gamma_3^-(\frac{1}{2}) - \Gamma_1^+$			
	D''	8.74	8.80	$\Lambda_3^- \rightarrow \Lambda_1^+$			
	D_1				8.28	8.24	Γ exciton
	D_1'				8.70	8.72	$\Gamma_3^- \rightarrow \Gamma_1^+$ gap
	D_2				8.92	8.84	Z exciton
	D_2'				9.82	9.73	$Z_3^- \rightarrow Z_1^+$
E		9.69	9.58	$Z_3^- \rightarrow Z_1^+$	10.19	10.19	$F_2^- \rightarrow F_1^+$
							$B_2 \rightarrow B_1$
F		10.58	10.38	$F_2^- \rightarrow F_1^+$			

V. CONCLUSIONS

The optical spectra of nickel dihalides have been divided into charge transfer, interband scattering, and excitonic structure. The charge-transfer transitions from the p -type valence band to the quasilocalized $3d^n$ states have been interpreted by means of a mixed-band localized-state model, deduced empirically by considering valence-band photoemission and optical spectra. The scattering region of the layered nickel halides is found to be somewhat similar to that of the isotropic alkali halides, and does not show evidence of bidimensional effects. The presented assignments to valence-to-conduction transitions for NiCl_2 agree fairly well with the available one-electron band calculation, once the band-gap value has been empirically adjusted. The exciton structure, which contains peaks overlapping the scattering continuum, is assigned, and the correct order of magnitude for the binding energy is found. The exciton line shape is explained by considering the interference effects between the exciton resonances and the scattering background. Finally, the interpretation of the satellite exciton at 6.5 eV in NiBr_2 is discussed, and reasonable arguments for its appearance only in transition-metal bromides are

given. In conclusion, we may say that while most of the optical spectra seem now to be satisfactorily interpreted on the basis of the available experimental data and theoretical efforts, we feel nonetheless that we cannot proceed much further until more experimental data (study of the excitonic and interband region of TM iodides; angular photoemission spectra in order to check the uppermost valence band) are collected and the theoretical picture is better established.

ACKNOWLEDGMENTS

The authors thank the technical staff of the Laboratoire d'Utilisation du Rayonnement Electromagnétique, as well as the members of the Laboratoire de l'Accélérateur Linéaire (Orsay), for their assistance during the course of experiments. The manuscript was prepared while one of us (I.P.) was visiting the University of Rennes. It is a pleasure for him to thank the staff of the Laboratoire de Spectroscopie for their hospitality. This work was also partially presented at the Second General Conference of the Condensed Matter Division of the European Physical Society, Manchester, U.K., proceedings edited by V. Heine (European Physical Society, Cambridge, 1982), Vol. 6A, p. 425.

-
- ¹D. Adler, in *Solid State Physics*, edited by F. Seitz, D. Turnbull, and H. Ehrenreich (Academic, New York, 1968), Vol. 21, p. 1.
- ²J. W. Allen, in *Magnetic Oxides*, edited by D. J. Craik (Wiley, New York, 1975), p. 349.
- ³R. J. Powell and W. E. Spicer, *Phys. Rev. B* **2**, 2182 (1970).
- ⁴L. Martin, A. Couget, and F. Pradal, *C.R. Acad. Sci.* **273**, 873 (1971).
- ⁵T. Ishii, Y. Sakisaka, T. Matsukawa, S. Sato, and T. Sagawa, *Solid State Commun.* **13**, 281 (1973); Y. Sakisaka, T. Ishii, and T. Sagawa, *J. Phys. Soc. Jpn.* **36**, 1372 (1974).
- ⁶I. Pollini and G. Spinolo, *J. Phys. C* **7**, 2391 (1974); G. Guizzetti, L. Nosenzo, I. Pollini, E. Reguzzoni, G. Samoggia, and G. Spinolo, *Phys. Rev. B* **14**, 4622 (1976).
- ⁷J. Thomas, G. Jezequel, and J. C. Lemonnier, in *VI International Conference on Vacuum Ultraviolet Radiation Physics, Charlottesville, Virginia, 1980*, Extended Abstract, Vol. I: Solid State Physics, I-46 (1980).
- ⁸D. Adler and J. Feinleib, *Phys. Rev. B* **2**, 3112 (1970).
- ⁹S. Antoci and L. Mihich, *Phys. Rev. B* **18**, 5768 (1978); *Solid State Commun.* **31**, 861 (1979).
- ¹⁰S. Antoci and L. Mihich, *Phys. Rev. B* **21**, 3383 (1980).
- ¹¹S. Hufner and G. K. Wertheim, *Phys. Rev. B* **8**, 4857 (1973).
- ¹²Y. Sakisaka, T. Ishii, and T. Sagawa, *J. Phys. Soc. Jpn.* **36**, 1372 (1974).
- ¹³J. Thomas, G. Jezequel, J. C. Lemonnier, I. Pollini, and R. Mamy (unpublished).
- ¹⁴R. W. G. Wyckoff, *Crystal Structure* (Interscience, New York, 1964).
- ¹⁵L. Messick, W. C. Walker, and R. Glosser, *Phys. Rev. B* **6**, 3941 (1972).
- ¹⁶J. L. McNatt, *Phys. Rev. Lett.* **21**, 1010 (1968).
- ¹⁷R. Glosser and W. C. Walker, *Solid State Commun.* **9**, 1599 (1971).
- ¹⁸M. Cardona, in *Solid State Physics*, edited by F. Seitz, D. Turnbull, and H. Ehrenreich (Academic, New York, 1969), Suppl. 11.
- ¹⁹J. Simonetti and D. S. McClure, *J. Chem. Phys.* **71**, 793 (1979).
- ²⁰F. Brown, C. Gahwiller, and A. B. Kunz, *Solid State Commun.* **9**, 487 (1971).
- ²¹H. R. Philipp and H. Ehrenreich, *Phys. Rev.* **131**, 2016 (1963).
- ²²I. Pollini, G. Spinolo, and G. Benedek, *Phys. Rev. B* **22**, 6369 (1980).
- ²³C. Kittel, *Introduction to Solid State Physics*, 4th ed. (Wiley, New York, 1971), p. 124.
- ²⁴J. E. Eby, K. J. Teegarden, and D. B. Dutton, *Phys. Rev.* **116**, 1099 (1959); K. Teegarden and G. Baldini, *ibid.* **155**, 896 (1967).
- ²⁵M. Cardona, *Phys. Rev.* **129**, 69 (1963); F. Bassani, R. S. Knox, and W. B. Fowler, *Phys. Rev. A* **137**, 1217 (1965).
- ²⁶D. K. Wright and M. R. Tubbs, *Phys. Status Solidi* **37**,

- 551 (1970).
- ²⁷D. L. Greenaway and R. Nitsche, *J. Phys. Chem. Solids* **26**, 1445 (1965).
- ²⁸U. Fano, *Phys. Rev.* **124**, 1866 (1961).
- ²⁹G. Harbeke, *Phys. Status Solidi* **27**, 9 (1968).
- ³⁰J. J. Hopfield, *J. Phys. Chem. Solids* **22**, 63 (1961).
- ³¹Y. Onodera and Y. Toyozawa, *J. Phys. Soc. Jpn.* **22**, 833 (1967).
- ³²J. C. Philipps, *Phys. Rev.* **136**, A1705 (1964).
- ³³D. L. Greenaway and G. Harbeke, *Optical Properties and Band Structure of Semiconductors* (Pergamon, New York, 1968), p. 123.
- ³⁴C. B. Duke and B. Segall, *Phys. Rev. Lett.* **17**, 19 (1966).
- ³⁵B. Velicky and J. Sak, *Phys. Status Solidi* **16**, 147 (1966).
- ³⁶J. Hermanson, *Phys. Rev. Lett.* **18**, 170 (1967), and references therein.
- ³⁷E. O. Kane, *Phys. Rev.* **180**, 852 (1969).
- ³⁸F. Bassani and G. Pastori Parravicini, *Electronic States and Optical Transitions in Solids* (Pergamon, New York, 1975), p. 196.